Available online at www.sciencedirect.com

ScienceDirect

IFAC Papers Online CONFERENCE PAPER ARCHIVE

IFAC PapersOnLine 50-1 (2017) 14705–14710

Real-Time Passive Control of Wave Energy Converters Using the Hilbert-Huang Transform ⋆

Paula B. Garcia-Rosa * **Geir Kulia** **
John V. Ringwood *** **Marta Molinas** *

* *Department of Engineering Cybernetics, Norwegian University of Science and Technology, Trondheim 7491, Norway (e-mails: p.b.garcia-rosa@ieee.org; marta.molinas@ntnu.no).*
** *Signal Analysis Lab AS, Olav Tryggvasons gate 27, Trondheim 7011, Norway (e-mail: geir.kulia@signalanalysislab.com)*
*** *Centre for Ocean Energy Research, Department of Electronic Engineering, Maynooth University, Co. Kildare, Ireland, (e-mail: john.ringwood@eeng.nuim.ie)*

Abstract: Passive loading is a suboptimal method of control for wave energy converters (WECs) that usually consists of tuning the power take-off (PTO) damping of the WEC to either the energy or the peak frequency of the local wave spectrum. Such approach results in a good solution for waves characterized by one-peak narrowband spectra. Nonetheless, real ocean waves are non-stationary by nature, and sea wave profiles with different spectral distribution occur in a specific location over time. Thus, the average energy absorption of passively controlled WECs tends to be low. In this paper, we propose a real-time passive control (PC) based on the Hilbert-Huang transform (HHT), where the PTO damping is time-varying and tuned to the instantaneous frequency of the wave excitation force. The instantaneous frequency is calculated by using the HHT, an analysis method for nonlinear and non-stationary signals that relies on the local characteristic time-scale of the signal. A performance comparison (in terms of energy absorption) of the proposed solution with the passive loading method is presented for a heaving system, in a variety of wave spectra. It is shown that a performance improvement of up to 21%, or 65%, is obtained for the proposed PC scheme, when it is compared to passive loading tuned to the energy, or the peak frequency of the spectrum, respectively. Real ocean waves off the west coast of Ireland are adopted in the simulations.

Keywords: Wave energy, renewable energy systems, control applications, suboptimal control, Hilbert-Huang transform.

1. INTRODUCTION

Currently, a number of studies have been done on the application of control technology to maximize energy capture of wave energy converters (WECs), see, e.g., Ringwood et al. (2014) for a literature overview of WEC control algorithms. Regardless of the strategy adopted, optimal hydrodynamic control requires a power take-off (PTO) system able to implement bidirectional power flow, since power has to be injected back into the WEC for some parts of the cycle. Passive loading, latching control and declutching are alternative methods of suboptimal control that avoid the need for the PTO to supply power.

Passive loading consists of tuning the PTO damping of the WEC to the predominant wave frequency of the local sea wave profile. Usually, the frequency selected is either the peak or the energy frequency of the wave spectrum (Yavuz et al., 2007; Garcia-Rosa et al., 2015). Furthermore, other studies optimize the damping by performing simulations with a range of possible values for each sea state adopted (Oskamp and Özkan Haller, 2012; Sjolte et al., 2013). Nonetheless, for irregular waves, the energy absorbed by passively controlled WECs are lower than other suboptimal control strategies like latching control (Bjarte-Larsson and Falnes, 2006; Hals et al., 2011; Garcia-Rosa et al., 2015). Conversely, Tom and Yeung (2014) have shown that for a passive control (PC) method where the PTO damping is time-varying, and obtained through a nonlinear model predictive controller, a great improvement in the energy absorption can be obtained over constant damping.

In this paper, we adopt a passive control approach where the PTO damping is time-varying and tuned to the instantaneous frequency of the wave excitation force. Due to the non-stationary nature of real ocean waves, we propose the Hilbert-Huang transform (HHT) (Huang et al., 1998) to calculate the instantaneous frequency. The HHT is an analysis method for nonlinear and non-stationary signals based on the Empirical Mode Decomposition (EMD). Different from methods that are based on the Fourier

⋆ This work was partially supported by CNPq-Brazil under grant number 201773/2015-5.

10.1016/j.ifacol.2017.08.2502

expansion, where the decomposition has a priori basis (trigonometric functions) and a global sense, the EMD has an adaptive basis and relies on the local characteristic time-scale of the signal. Thus, the EMD can extract the different oscillation modes (named as Intrinsic Mode Functions, IMFs) present in a wave profile.

The aim is to verify the energy content of the IMF components of the wave excitation force, identify the dominant component and use the information of its instantaneous frequency in the PC approach. A performance comparison (in terms of energy absorption) of the proposed solution with passive loading is presented for a heaving system with one degree of freedom, in a variety of real wave profiles. Real ocean waves off the west coast of Ireland are adopted in the simulations. A comparison of the energy absorption for constant PTO damping tuned at different frequencies, namely, the energy and peak frequency of the spectrum, is also presented.

2. DYNAMIC MODELING OF THE WEC

Figure 1 illustrates the WEC considered in this paper. The WEC is a single oscillating-body represented as a truncated vertical cylinder with a generic PTO system. The wetted surface of the cylinder is defined by a draught d and a radius r.

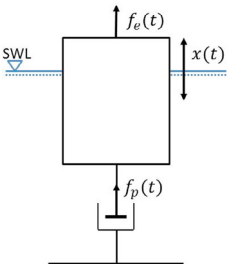

Fig. 1. Schematic of the generic heaving floating body.

2.1 Equation of Motion

Here, we assume linear hydrodynamic theory and heave oscillatory motion of the WEC. In such a case, the motion of the floating body is described by

$$m\ddot{x}(t) = f_e(t) + f_r(t) + f_s(t) + f_p(t)\,, \tag{1}$$

where $x \in \mathbb{R}$ is the vertical position of the body, $m \in \mathbb{R}_+$ is the body mass, $f_s = Sx$ is the restoring force, $S \in \mathbb{R}_+$ is the buoyancy stiffness, f_p is the force applied by the PTO mechanism, f_e is the excitation force on the body held fixed in incident waves, and f_r is the radiation force due to the body oscillation in the absence of waves.

From Cummins (1962),

$$-f_r(t) = m_r(\infty)\,\ddot{x} + \int_0^t h_r(t-\tau)\,\dot{x}(\tau)\,d\tau\,, \tag{2}$$

where $m_r(\infty) \in \mathbb{R}_+$ is the infinite-frequency added mass coefficient, defined with the asymptotic values of the added masses at infinite frequency. The kernel of the convolution term $h_r(t-\tau)$ is known as the fluid memory term:

$$h_r(t) = \frac{2}{\pi}\int_0^\infty B_r(\omega)\cos(\omega t - \tau)\,d\omega\,, \tag{3}$$

where $B_r(\omega) \in \mathbb{R}_+$ is the radiation damping coefficient, and $\omega \in \mathbb{R}_+$ is the wave frequency. Thus, the vertical motion of the floating body (1) becomes

$$M\ddot{x}(t) + \int_0^t h_r(t-\tau)\,\dot{x}(\tau)\,d\tau + Sx(t) = f_e(t) + f_p(t)\,, \tag{4}$$

with $M = [m + m_r(\infty)]$. The excitation force is given by

$$f_e(t) = \int_{-\infty}^{\infty} h_e(t-\tau)\,\zeta(\tau)\,d\tau\,, \tag{5}$$

where

$$h_e(t) = \frac{1}{2\pi}\int_{-\infty}^{\infty} H_e(\omega)e^{i\omega t}\,d\omega\,, \tag{6}$$

is the inverse Fourier transform of the excitation force transfer function $H_e(\omega)$, and ζ is the wave elevation. $H_e(\omega)$ is a property of the floating body and has low-pass filter characteristics. Notice that (6) is non-causal, since in fact, the pressure distribution is the cause of the force and not the incident waves (Falnes, 2002). Furthermore, real ocean waves are usually characterized by their energy density spectrum $S(\omega)$. Following the linear approach, the spectrum of the excitation force is

$$S_{fe}(\omega) = |H_e(\omega)|^2 S(\omega)\,. \tag{7}$$

A generic PTO system with a damper ($B_p \in \mathbb{R}_+$) varying in time is adopted. The PTO force is parameterized as a function of the body velocity $\dot{x}(t)$:

$$f_p(t) = B_p(t)\dot{x}(t)\,. \tag{8}$$

The extracted energy, and the mean extracted power by the WEC over a time range T are, respectively,

$$E_a = -\int_0^T \dot{x}(t) f_p(t) dt\,, \tag{9}$$

$$P_a = \frac{E_a}{T}\,. \tag{10}$$

2.2 Optimal Conditions for Maximum Wave Energy Extraction

For regular wave regime (waves defined by a single frequency) and for $B_p(t) = B_p$ for any time t, Falnes (2002) has shown that maximum absorption is obtained when

$$B_p = \sqrt{(B_r(\omega))^2 + (\omega(m + m_r(\omega)) - S/\omega)^2}\,, \tag{11}$$

where $m_r(\omega) \in \mathbb{R}$ is the added mass. Furthermore, if m and S can be chosen such that

$$(m + m_r(\omega))\omega - S/\omega = 0\,, \tag{12}$$

then (11) becomes

$$B_p = B_r(\omega)\,. \tag{13}$$

Equation (11) is referred as optimum amplitude condition and (12) is referred as optimum phase condition (Falnes, 2002). The greatest wave energy absorption is obtained when both conditions are satisfied, and then the PTO damping is given by (13). In such a case, the velocity of the floating body is in phase with the excitation force (Falnes, 2002), and the PTO system should be able to implement bidirectional power flow.

Passive loading consists of setting the PTO damping B_p to a constant value. Equation (11) represents optimal linear damping when the floating body is subjected to incident regular waves. Since irregular waves and real ocean waves are not defined by a single frequency in the time domain, a common approach is to select a frequency that characterizes the wave spectrum for tuning the damping. Usually, the frequency selected is either the peak (ω_p) or the energy frequency (ω_e) of the wave spectrum. Different time scales can be applied for tuning the PTO damping: hourly basis (according to sea states variations), monthly basis (according to seasonal variations), or annually basis (Oskamp and Özkan Haller, 2012).

An alternative approach where the PTO damping (11) is modified on a wave-by-wave basis is presented next.

3. REAL-TIME PASSIVE CONTROL

3.1 Overview of the proposed control method

Since some of the high frequency content of the wave elevation is filtered by $H_e(\omega)$, we consider the instantaneous frequency of the excitation force in our real-time PC approach, rather than the instantaneous frequency of the waves.

The calculation of the instantaneous frequency by applying the Hilbert transform (HT) directly to $f_e(t)$ results in negative local frequencies, as the instantaneous frequency is not well defined for multi-component signals (Boashash, 1992), i.e. signals with more than one local extrema for each zero crossing. Thus, $f_e(t)$ is decomposed into mono-component signals (IMFs) using the EMD.

Here, we assume that the excitation force is known completely over the interval T. By applying the HHT approach, $f_e(t)$ can be expressed as

$$f_e(t) = \mathbb{R}\sum_{i=1}^{N} \hat{a}_i(t) e^{i\int \hat{\omega}_i(t)dt}\,, \tag{14}$$

where N is the total number of IMF components defined here as $N = \log_2 N_s - 1$ (Wu and Huang, 2004), N_s is the data length, $\hat{a}_i$ and $\hat{\omega}_i$ are respectively the amplitude and the instantaneous frequency of the i-th IMF component. Equation (14) is considered as a generalized form of the Fourier expansion, with both amplitude and frequency represented as functions of time (Huang et al., 1998).

The aim is to identify the dominant IMF component (in terms of the energy of the signal), and use the information of its instantaneous frequency for tuning the PTO damping. From (11),

$$B_p(t) = \sqrt{(B_r(\hat{\omega}_d))^2 + (\hat{\omega}_d(m + m_r(\hat{\omega}_d)) - S/\hat{\omega}_d)^2}\,. \tag{15}$$

where $\hat{\omega}_d$ is the instantaneous frequency of the dominant IMF component. Figure 2 illustrates the block diagram of the proposed real-time PC based on the HHT approach. The procedure to calculate $\hat{\omega}_d$ is described next.

3.2 Instantaneous frequency of the dominant IMF component

In order to determine $\hat{\omega}_d(t)$, firstly we decompose $f_e(t)$ into IMF components using the EMD. The EMD identifies local maxima and minima of the signal, and calculates upper and lower envelopes for these points by using cubic splines. The mean values of the envelopes are used to decompose the original signal into frequency components in a sequence from the highest frequency to the lowest one. The EMD procedure is summarized in the following algorithm:

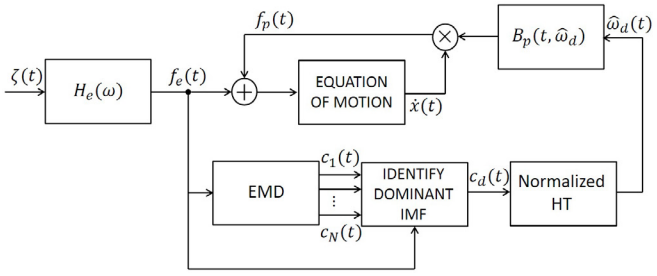

Fig. 2. Block diagram of the proposed PC.

Step 0: Set $i=1$; $r(t)=f_e(t)$;
Step 1: Identify the local maxima and minima in $r(t)$;
Step 2: Calculate the upper envelope defined by the maxima, and the lower envelope defined by the minima;
Step 3: Calculate the mean envelope $m(t)$;
Step 4: Set $h(t)=r(t)-m(t)$;
Step 5: If $h(t)$ is an IMF, go to next step. Otherwise, set $r(t)=h(t)$ and go back to step 1;
Step 6: Set $c_i(t)=h(t)$; $r(t)=r(t)-c_i(t)$;
Step 7: If $i = N$, define the IMF components as $c_1(t), ..., c_N(t)$, and the residue as $r(t)$. Otherwise, set $i=i+1$ and go back to step 1.

After the EMD, the dominant IMF is identified through the comparison of the energy of the IMF signals (E_{ci}) with the energy of the excitation force signal (E_{fe}),

$$E_{ci} = \int_0^T |c_i(t)|^2 dt\,, \tag{16}$$

$$E_{fe} = \int_0^T |f_e(t)|^2 dt\,, \tag{17}$$

where $c_i(t)$ is the i-th IMF component. The IMF with the highest ratio of energy content E_{ci}/E_{fe} is the dominant component $c_d(t)$.

Additionally, in order to avoid other limitations of the HT (Huang, 2005), the dominant IMF is normalized by dividing it by a spline envelope defined through all the maxima of the IMF, as described in Huang (2005).

Finally, the Hilbert transform is applied to the normalized dominant component $\bar{c}_d(t)$ (Huang et al., 1998):

$$\bar{v}_d(t) = \frac{1}{\pi} P \int_{-\infty}^{\infty} \frac{\bar{c}_d(\tau)}{t-\tau} d\tau\,, \tag{18}$$

where P indicates the Cauchy principal value, and $\bar{v}_d$ is the HT of $\bar{c}_d$. Then, the dominant IMF component is represented as an analytic signal

$$\bar{z}_d(t) = \bar{c}_d(t) + j\bar{v}_d(t) = \hat{a}_d(t) e^{i\int \hat{\omega}_d(t)dt}\,, \tag{19}$$

with amplitude $\hat{a}_d(t)$ and instantaneous frequency $\hat{\omega}_d(t)$ calculated by

$$\hat{a}_d(t) = \sqrt{\bar{c}_d^2(t) + \bar{v}_d^2(t)}\,, \tag{20}$$

$$\hat{\omega}_d(t) = \frac{d\phi_d(t)}{dt}\,, \tag{21}$$

where $\phi_d(t) = \arctan(\bar{v}_d(t)/\bar{c}_d(t))$.

4. SIMULATIONS

4.1 Hydrodynamic parameters

Here, we consider a heaving cylinder with radius $r = 5\,\text{m}$, draught $d = 4\,\text{m}$, and mass $m = 3.2 \times 10^5\,\text{kg}$. The hydrodynamic coefficients of the cylinder were computed using the boundary element solver WAMIT, Inc. (1998-2006). Figure 3 illustrates the added mass and radiation damping coefficients, and the frequency response of the excitation force.

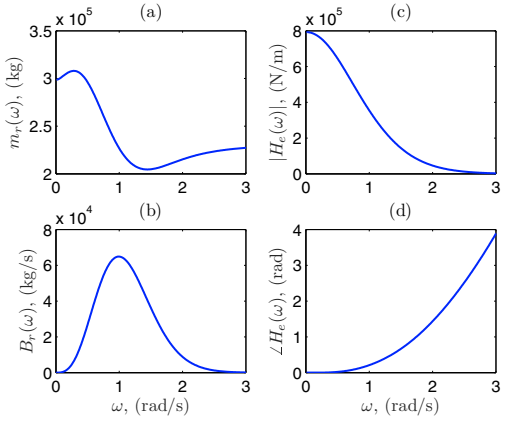

Fig. 3. Hydrodynamic data. (a) Added mass $m_r(\omega)$, (b) Radiation damping $B_r(\omega)$, (c) Magnitude $|H_e(\omega)|$ and (d) phase $\angle H_e(\omega)$ of the excitation force frequency response.

4.2 Real Wave Data

Real wave data provided by the Irish Marine Institute are adopted for the simulations. The data consists of wave elevation records of 30 minutes, sampled at 1.28 Hz, and it was collected in 2010 from a data buoy in the Belmullet wave energy test site, off the west coast of Ireland.

In order to verify the performance of the proposed controller, nine wave elevation records with different spectral distributions have been selected for our study. The selected records are referred as sea states S1-S9. Figure 4 illustrates the wave spectra of the sea states, and Table 1 shows the significant wave height H_s, the energy frequency ω_e, and the peak frequency ω_p of the spectra. The statistical parameters H_s and ω_e are respectively calculated as: $H_s = 4\sqrt{m_0}$, and $\omega_e = m_0/m_{-1}$, where $m_n = \int_0^\infty \omega^n S(\omega) d\omega$ is the spectral moment of order n. ω_p is the frequency at which the wave spectrum is maximum.

4.3 Simulation Results

Figure 5 shows the spectral density of the excitation force for the selected sea states. It can be noted that some of

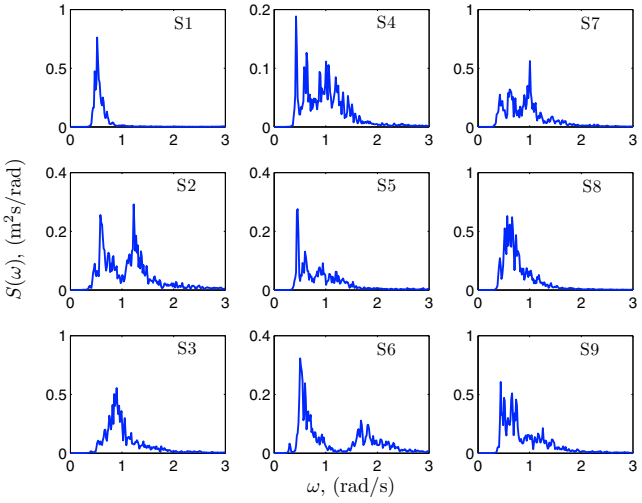

Fig. 4. Wave spectra of real wave data from Belmullet.

Table 1. Significant wave height H_s (m), energy frequency ω_e (rad/s), and peak frequency ω_p (rad/s) of the selected sea states.

	S1	S2	S3	S4	S5	S6	S7	S8	S9
H_s	1.26	1.43	1.80	1.06	1.06	1.35	1.80	1.88	1.90
ω_e	0.59	0.94	0.94	0.84	0.75	0.85	0.79	0.70	0.75
ω_p	0.52	1.22	0.90	0.42	0.46	0.50	1.01	0.57	0.44

the high frequency waves in Figure 4 are filtered out by the transfer function $H_e(\omega)$, that is defined by the shape of the floating body. Thus, the excitation force spectra are characteristic of the cylinder adopted in this study.

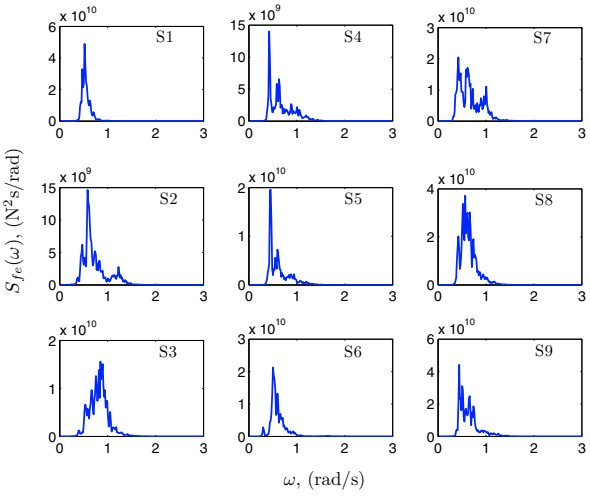

Fig. 5. Excitation force spectra.

A. Constant damping Firstly, we adopt the passive loading method, and the PTO damping is tuned either at ω_e or at ω_p. The energy absorbed by the WEC is denoted by E_{a,ω_e} and E_{a,ω_p} for the two cases, respectively. In order to compare the energy absorbed in such cases, Table 2 shows the ratio $E_{a,\omega_e}/E_{a,\omega_p}$.

For most of the studied cases, tuning the constant damping at ω_e gives greater energy capture than tuning at ω_p.

Table 2. Ratio of E_{a,ω_e} and E_{a,ω_p}.

S1	S2	S3	S4	S5	S6	S7	S8	S9
1.01	1.36	0.99	1.36	1.16	0.93	1.08	1.18	1.18

The highest differences in the absorption of energy are obtained for sea states S2 and S4. Both sea states are characterized by wideband spectra. Nonetheless, for S2 the high frequency peak ($\omega_p = 1.22$ rad/s) is filtered out by the shape of the body, as it is illustrated in Fig. 5.S2, which can explain tuning B_p at ω_e results in greater energy absorption than tuning at ω_p. In the sea state S4, the energy is spread from about 0.4 to 1.5 rad/s (Fig. 5.S4), and the low frequency peak ($\omega_p = 0.42$ rad/s) is half of the energy frequency ($\omega_e = 0.84$ rad/s).

B. Proposed control method The damping is varying in time and uses the instantaneous frequency information of the dominant IMF component for tuning purposes, as it is described in Section 3. The EMD procedure is applied to the excitation force signals, and the resultant ratios of the energy of the IMF signals (E_{ci}) and the energy of the excitation force signal (E_{fe}) are shown in Figure 6. Clearly, the IMF component c_1 is the dominant component for all cases, although in some cases, for instance the wideband spectra S2, S4, and S7, the signal energy of component c_2 is also significant (about 40% of E_{fe}).

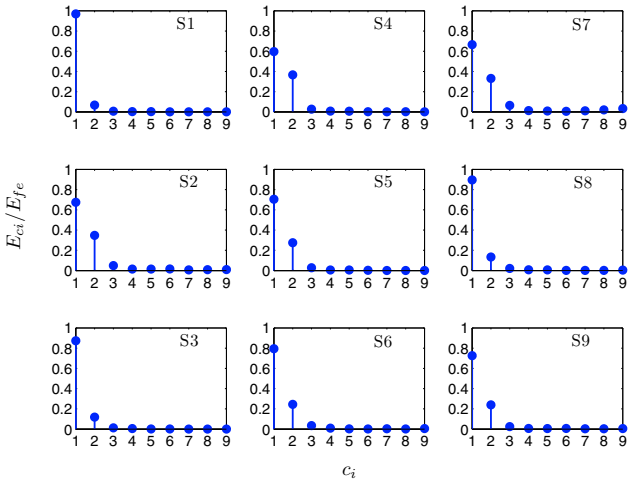

Fig. 6. Ratio of E_{ci} and E_{fe}.

In order to illustrate the effect of the proposed real-time PC in the variables of the system, Figure 7 shows samples of time-series simulations for the sea states S1 and S2. For S1, the evolution of the position x, and the PTO force f_p for the proposed controller are slightly different from the case when the damping is constant and tuned at ω_e. In such a case, the energy absorbed over a 30-min simulation (Fig. 8.a) is only 2.9% greater than the constant damping approach, whereas for S2 the improvement is more significant, about 21% greater than constant damping (Fig. 8.b), and the PTO force has higher peaks than the constant damping case (Fig. 7.b).

Such behaviour can be explained by the different energy spectral distributions of both sea states. S1 is characterized by a narrowband spectrum with a single dominant swell (low frequency waves generated in other locations), and then the energy is concentrated in a narrow band of frequencies, mostly around ω_e. However, S2 is characterized by a two-peak spectrum with mixed wind-sea (high frequency waves generated by the local wind) and swell conditions and then, the energy is spread over a wider band of frequencies than S1.

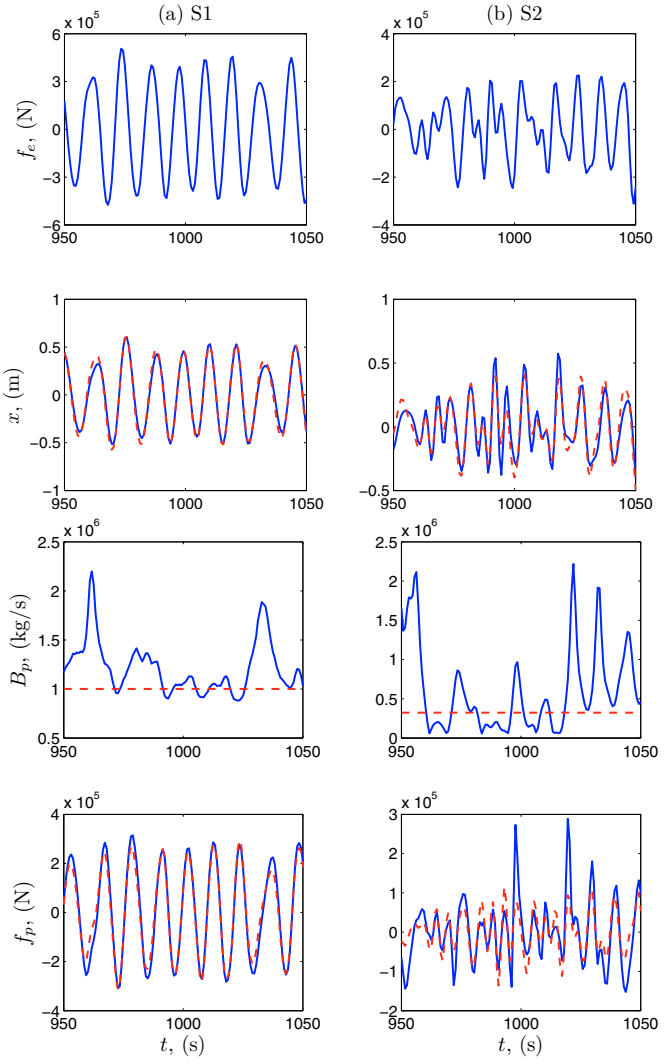

Fig. 7. Time-series of the excitation force, position, PTO damping, and PTO force for the proposed PC (solid line) and the passive loading approach (dashed line) (a) S1; (b) S2.

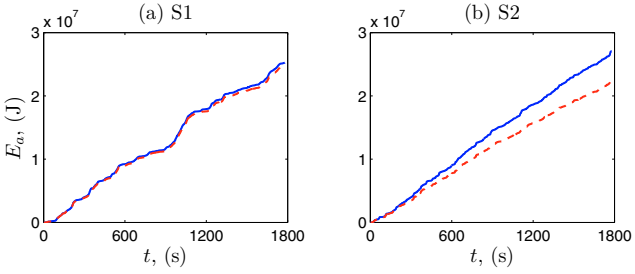

Fig. 8. Energy absorbed over a 30-min simulation for the proposed PC (solid line) and the passive loading approach (dashed line) (a) S1; (b) S2.

A comparison of the energy absorbed (E_a) by the WEC when the proposed control scheme is adopted and when passive loading is adopted is illustrated in Figure 9. For the passive loading approach, the PTO damping is tuned either at ω_e or at ω_p. The energy capture for the proposed controller is superior to passive loading in all studied cases. A performance improvement in the absorbed energy from 2.9% to 21% is obtained when it is compared with constant damping tuned at ω_e, and from 3.6% to 65% when the damping is tuned at ω_p.

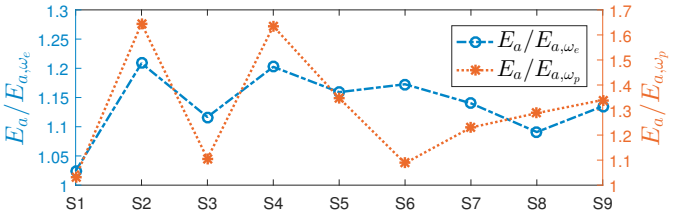

Fig. 9. Ratios between E_a and E_{a,ω_e}, and E_a and E_{a,ω_p}.

5. CONCLUSION

When real ocean waves and the passive loading method are adopted, tuning the constant damping at the energy frequency of the wave spectrum usually results in greater absorption of energy than tuning it at the peak frequency. The excitation force spectrum filters out some of the high frequency components of the wave spectrum. The filtering characteristics depend on the shape of the body.

A real-time passive control based on the Hilbert-Huang transform has been proposed to improve the energy absorption of WECs that cannot implement bidirectional power flow. For the studied sea states, an average energy improvement of 15%, and 29%, is obtained for the proposed control when it is compared with the constant damping respectively tuned at the energy, and the peak frequency of the wave spectrum. The lowest improvements are obtained for the sea state characterized by a narrowband spectrum with energy concentrated at a single dominant swell.

The proposed controller is suboptimal, as it considers only the dominant IMF component of the excitation force. To further improve the energy absorption, a scheme adopting more than one IMF component could be developed. Such scheme would be specially beneficial for the cases where the second IMF is also significant, as characterized by some of the wideband spectra adopted in this study.

Furthermore, the proposed controller requires higher PTO forces than the constant damping approach. For practical application studies, constraints on the position of the body and on the PTO force should be taken into account. A scheme similar to the constrained control from Fusco and Ringwood (2013) could be adopted.

ACKNOWLEDGEMENTS

The authors would like to acknowledge the Irish Marine Institute for providing the wave data from the Belmullet test site, and Lars Lundheim for the useful discussions while implementing the HHT software. Special thanks are in order to Norden Huang for personally giving insight into his methods. His open-mindedness and generosity have been highly appreciated.

REFERENCES

Bjarte-Larsson, T. and Falnes, J. (2006). Laboratory experiment on heaving body with hydraulic power take-off and latching control. *Ocean Engineering*, 33(7), 847–877.

Boashash, B. (1992). Estimating and interpreting the instantaneous frequency of a signal - Part 1: Fundamentals. *Proc. of the IEEE*, 80(4), 520–538.

Cummins, W.E. (1962). The impulse response function and ship motions. *Schiffstechnik*, 47(9), 101–109.

Falnes, J. (2002). *Ocean Waves and Oscillating Systems: Linear Interaction including Wave-Energy Extraction.* Cambridge University Press, USA.

Fusco, F. and Ringwood, J.V. (2013). A simple and effective real-time controller for wave energy converters. *IEEE Trans. on Sustainable Energy*, 4(1), 21–30.

Garcia-Rosa, P.B., Bacelli, G., and Ringwood, J.V. (2015). Control-informed geometric optimization of wave energy converters: The impact of device motion and force constraints. *Energies*, 8(12), 13672–13687.

Hals, J., Falnes, J., and Moan, T. (2011). A comparison of selected strategies for adaptive control of wave energy converters. *J. of Offshore Mech. and Arct. Eng.*, 133(3), 031101–031113.

Huang, N.E. (2005). *Introduction to Hilbert-Huang Transform and some recent developments. The Hilbert-Huang Transform in Engineering.* CRC Press. Edited by N. E. Huang and N. O. Attoh-Okine, 1–23.

Huang, N.E., Shen, Z., Long, S.R., Wu, M.C., Shih, H.H., Zheng, Q., Yen, N.C., Tung, C.C., and Liu, H.H. (1998). The empirical mode decomposition and the Hilbert spectrum for nonlinear and non-stationary time series analysis. *Proc. Royal Society London*, 454, 903–995.

Oskamp, J.A. and Özkan Haller, H.T. (2012). Power calculations for a passively tuned point absorber wave energy converter on the Oregon coast. *Renewable Energy*, 45, 72–77.

Ringwood, J.V., Bacelli, G., and Fusco, F. (2014). Energy-maximizing control of wave-energy converters. *IEEE Control Systems Magazine*, 34(5), 30–55.

Sjolte, J., Sandvik, C.M., Tedeschi, E., and Molinas, M. (2013). Exploring the potential for increased production from the wave energy converter Lifesaver by reactive control. *Energies*, 6(8), 3706–3733.

Tom, N. and Yeung, R.W. (2014). Nonlinear model predictive control applied to a generic ocean-wave energy extractor. *J. Offshore Mech. Arct. Eng.*, 136(4).

WAMIT, Inc. (1998-2006). *WAMIT User Manual Versions 6.4, 6.4PC and 6.3S, 6.3S-PC.* USA.

Wu, Z. and Huang, N.E. (2004). A study of the characteristics of white noise using the empirical mode decomposition method. *Proc. Royal Society London*, 460, 1597–1611.

Yavuz, H., Stallard, T.J., McCabe, A.P., and Aggidis, G.A. (2007). Time series analysis-based adaptive tuning techniques for a heaving wave energy converter in irregular seas. *Proc. of the Inst. of Mech. Engineers, Part A: Journal of Power and Energy*, 221(1), 77–90.